Beneficial Effect of Indigo Naturalis on Acute Lung Injury Induced by Influenza a Virus

Peng Tu
Fudan University School of Pharmacy
Rong Tian
Fudan University School of Pharmacy
Yan Lu
Fudan University School of Pharmacy
Yunyi Zhang
Fudan University School of Pharmacy
Haiyan Zhu
Fudan University School of Pharmacy
Lijun Ling
Fudan University School of Pharmacy
Hong Li
Fudan University School of Pharmacy
Daofeng Chen (dfchen@shmu.edu.cn)
Fudan University School of Pharmacy

Research

Keywords: influenza, indigo naturalis, acute lune injury, cytokines, COVID-19

Posted Date: September 8th, 2020

DOI: https://doi.org/10.21203/rs.3.rs-73166/v1

Version of Record: A version of this preprint was published on December 21st, 2020. See the published version at https://doi.org/10.1186/s13020-020-00415-w.

Abstract

Background: Infections induced by influenza viruses, as well as COVID-19 pandemic induced by SARS-CoV-2 led to Acute lung injury (ALI) and multiorgan failure, during which traditional Chinese medicine played an important role in treatment of the pandemic. The study aimed to investigate the effect of indigo naturalis on ALI induced by influenza A virus (IAV) in mice.

Method: The anti-influenza and anti-inflammatory properties of aqueous extracts of indigo naturalis (INAE) were evaluated *in vitro*. BALB/c mice inoculated intranasally with IAV (H1N1) were treated intragastrically with INAE (40, 80 and 160 mg kg^{-1}/d) 2 h later for 4 or 7 days. Animal mortality and lifespan were recorded. Expression of high mobility group box-1 protein (HMGB-1) and toll-like receptor-4 (TLR4) were evaluated through immunohistological staining. Inflammatory cytokines were also monitored by ELISA.

Result: INAE inhibited virus growth on Madin-Darby canine kidney (MDCK) cells and decreased nitric oxide (NO) production from lipopolysaccharide (LPS)-stimulated peritoneal macrophage *in vitro*. The results showed that oral administration of 160 mg/kg of INAE significantly improved the lifespan ($P < 0.01$) and survival rate of IAV infected mice, improved lung injury and lowered viral replication in lung tissue ($P < 0.01$). Treatment with INAE (40, 80 and 160 mg/kg) also significantly increased liver weight and liver index ($P < 0.05$), as well as spleen and thymus weight and organ index at 160 mg/kg ($P < 0.05$). The expression of HMGB-1 and TLR4 in lung tissue were also suppressed. Treatment with INAE reduced the high levels of interferon α (IFN-α), interferon β (IFN-β), interferon γ (IFN-γ), monocyte chemoattractant protein-1 (MCP-1), regulated upon activation normal T cell expressed and secreted factor (RANTES), interferon induced protein-10 (IP-10), tumor necrosis factor-α (TNF-α), interleukin-6 (IL-6) ($P < 0.05$), with increased production of interleukin-10 (IL-10) ($P < 0.05$). The increased myeloperoxidase (MPO) activity and methylene dioxyamphetamine (MDA) level in lung tissues were inhibited by INAE treatment ($P < 0.05$).

Conclusion: The results showed that INae alleviated IAV induced ALI in mice. The effect of INAE might be related with its anti-virus, anti-inflammatory and anti-oxidation properties, which give a hint that indigo naturalis might be effective on respiratory viruses infected acute lung injury or SAR-CoV-2 caused COVID-19.

Background

The current outbreak of COVID-19 emerged in December 2019, Wuhan, the geographic center of China and has spread from China to other countries, with more than 26 billion cases and 80 thousand death up to date [1]. The growing infections is second only to the influenza virus infection occurred in1918, which killed more than 50 billion people worldwide, and resulted in havoc with military operations during the First World War [2]. Influenza A virus (IAV) is one of important human pathogens worldwide. IAV infection may cause severe lung injury, such as acute respiratory distress syndrome (ARDS), pneumonia, and lead

to high mortality and morbidity [3]. Just like the current coronavirus pandemic which is spreading surpass 200 countries and regions, fast spread of IAV infection may cause epidemic and threat people's safety and property [4].

IAV is negative strand RNA virus belonging to the family of orthomyxoviridae with a genome consisting of eight single stranded RNA segments of negative polarity [5, 6]. Vaccine, M2 ion channel inhibitors and neuraminidase inhibitors are most used for treatment of IAV infection [7]. However, the lack of timeliness of vaccines and continuous records about drug resistance to influenza virus impetus the demands for new alternative antivirus substance, especially from nature products and traditional Chinese medicine [8].

Acute lung injury (ALI) is characterized by severe lung edema and inflammation, and the pathogenesis of ALI involves immune imbalance [9]. During the process of IAV infection, high mobility group box-1 protein (HMGB-1) were released from the injured cells in lung. The binding of HMGB-1 to the toll-like receptor 4 (TLR4), as well as the recruitment of neutrophils to the infected areas accelerated the production of large amount of oxidative products and proinflammatory cytokines, and further aggravated lung injury [10, 11]. Influenza virus infection and COVID-19 both result in respiratory system symptom and perhaps share similar infection process. Besides pneumonia and acute lung injury, other vital organs injury, such as liver, thymus, spleen, heart or kidneys dysfunction were observed in patient suffered from COVID-19 [12].

Traditional Chinese medicine (TCM), the precious treasure of China which stem from antique Chinese culture 2000 years ago, are used to treat diseases in southeast Asia and many other countries [13]. TCM played significant role in the treatment of COVID-19, bringing new hope for the prevention and control of COVID-19 and influenza virus [14].

Indigo naturalis, a dark blue powder, mass or granules, is prepared from stems and leaves of *Baphicacanthus cusia* (Nees) Bremek. (Fam. Acanthaceae)*, Polygonum tinctorium* Ait. (Fam. Polygonaceae) *orlsatis indigotica* Fort. (Fam Cruciferae) [15, 16]. Indigo naturalis is a folk traditional Chinese medicine, which is used to treat psoriasis, colitis and upper respiratory system diseases [17]. Traditional Chinese medicine exhibited effective therapeutic capacity during SARS pandemic in 2003 and amid COVID-19 outbreak in 2020. We supposed that indigo naturalis*,* which is effective in respiratory system diseases, perhaps can alleviate lung injury induced by IAV infection.

As of today, no studies were reported regarding the therapeutic effect of indigo naturalis. In our study, aqueous extract of indigo naturalis (INAE) was prepared and analyzed. The anti-influenza and anti-inflammatory effects of INAE were evaluated both *in vitro* and *in vivo*. The role and potential mechanism of INAE against H1N1 influenza viruses induced ALI was explored in this study.

Methods

Reagent

The powdered form of Indigo naturalis was prepared from the leaves of *B. cusia* (Nees) Bremek and purchased from Shanghai Ley's Pharmaceutical Co., Ltd., with the place of production of Xianyou county, Fujian province, China. The material was identified and authenticated by Dr. Daofeng Chen, chief of Department of Natural Medicine, School of Pharmacy, Fudan University. The voucher specimen of indigo naturalis (DFC-LF-201509) was deposited in Department of Natural Medicine, School of Pharmacy, Fudan University.

Ribavirin was purchased from Shanghai Meryer chemical Co., Ltd.. ELISA kits for mouse tumor necrosis factor-α (TNF-α), interleukin-6 (IL-6), monocyte chemoattractant protein-1 (MCP-1), regulated upon activation normal T cell expressed and secreted factor (RANTES), interleukin-10 (IL-10), and interferon induced protein-10 (IP-10) were purchased from Shanghai Boatman Biotechnology Co. Ltd.. ELISA kits for interferon-α (IFN-α), interferon β (IFN-β), interferon γ (IFN-γ), myeloperoxidase (MPO), methylene dioxyamphetamine (MDA) were purchased from Shanghai Beyotime Biotechnology Co., Ltd.. The anti-HMGB-1 and anti-TLR4 antibodies were purchased from Abcam (San Francisco, CA, USA).

Herbal extract preparation

The indigo naturalis powder (2 kg) were packaged with 4 layers of etamine, and then extracted with boiling water for 1 h with three times. The water extract was concentrated under reduced pressure and lyophilized to produce 82 g of aqueous extract of indigo naturalis (INAE).

In vitro antiviral evaluation

The influenza A virus (H1N1 A/FM/1/47) was denoted by vice professor Haiyan Zhu, department of microbiological and biochemical pharmacy, school of pharmacy, Fudan University. According to the reference and procedures in our lab, the virus was suspended in Dulbecco's modified Eagle's medium (DMEM), propagated in lung of mice and stored at -80°C. The 50% lethal dose (LD_{50}) of virus was determined in mice infected with serial dilutions of virus [18].

In vitro antiviral evaluation was conducted as described with minor modification [19]. Madin-Darby canine kidney (MDCK) cells were cultured in DMEM supplemented with 10% fetal bovine serum (Hyclone, CA, USA), streptomycin and penicillin. Briefly, MDCK cells were cultured in 96-well plates (1×10^5 cells per well) till cells fulfilled 90% percent of the bottom. INAE were diluted and prepared in concentrations of 0, 10, 25, 50, 100, 200 and 400 μg/mL. The antiviral process was investigated based on three ways of action: added the drugs 2 h before, incubated the drugs with 100 TCID 50 influenza, or 2 h after virus infection. The cells with only infection viruses were served as virus control. After 3 days incubation, 3-(4,5-dimethyl-2-thiazolyl)-2,5-diphenyl-2-H-tetrazolium bromide (MTT) was added into the wells. Following 4 h incubation, the optical density value (OD value) of supernatant was tested. Inhibition rate (%) = [(OD of INAE – mean OD of virus control) / (mean OD of cells control - mean OD of virus control)] × 100%.

In vitro anti-inflammatory effect

BALB/c mice were administrated with 5% mercaptoethanol acid sodium by intra-peritoneal injection and scarified 4 days later to harvest peritoneal macrophages. Macrophages were suspended with RPMI-1640 culture medium containing 10% fetal bovine serum and antibiotics. The cells were cultured in 96 cell plate (1×10^6 cells per well) for 2 h. The serial dilutions of INAE, lipopolysaccharide (LPS, 1 μg/ml), and dexamethasone (positive control, 10 μM) were added and incubated for 24 h. A sample of cells without LPS was set aside to serve as a control. The supernatant was collected at the end of the incubation. Nitrogen oxide (NO) production in the peritoneal macrophage was determined by measuring the OD value of supernatant following the instruction of method using Griess reagent [20].

animals

Specific pathogen-free male BALB/c mice (14 ~ 16 g) were purchased from Shanghai SLAC Laboratory Animal Co., Ltd. [SCXK (Hu) 2012-0002]. The mice were housed in collective cages under a 12 h light/dark room, with free access to food and water. The air temperature was maintained at 22 ± 2°C with relative humidity of 50 ± 10%. Experiments were carried out according to the guideline for the care of laboratory animals of national institutes of health. All study protocols were approved by the animal ethical committee of school of pharmacy, Fudan University (approval No. 2015-10-SY-CDF-01).

Survival experiment in IAV infected mice

The survival experiment was conducted as described with minor modification [21]. Mice were randomly divided into six groups (n = 10): normal, model, INAE (40, 80 and 160 mg/kg) and positive control (ribavirin,100 mg/kg). Mice were anaesthetized by tail intravenous injection of propofol (0.026 mL/10g) and were intranasal challenged with 6 × LD50 IAV in 30 μL DMEM 2 h before treatment. Normal mice were challenged with 30 μL DMEM. The mice were treated orally with INAE or ribavirin once daily for 7 days. For comparison, normal group and model group were given 0.5% carboxymethyl cellulose sodium (CMC-Na). All groups were monitored for 14 days after virus infection. Body weight, body temperature, and numbers of mice were recorded daily. Lifespan and mortality rate of mice were calculated.

Acute lung injury in IAV infected mice

The experiment was scheduled by six groups (n = 6): normal, model, INAE (40, 80 and 160 mg/kg) and positive control (ribavirin,100 mg/kg). Mice were challenged with $3 \times LD_{50}$ IAV in 30 μL DMEM 2 h before treatment. Normal mice were challenged with 30 μL DMEM. The mice were orally treated with agents as we mentioned about. The treatment began 2 h after the virus challenge and once daily for 4 days. The mice were sacrificed on the 4^{th} day post infection. The lung tissues were harvested, weighted and then washed with pre-chilled saline. The superior right lobe was cut and placed in 10% neutral formalin buffer for histopathologic evaluation, and the rest parts were snap frozen at -80°C for cytokines detection [22]. To estimate the severity of lung, liver, thymus and spleen. Organ indexes were calculated as follows: Organs index = Organ weight (mg) / body weight (g) × 100%.

Lung tissues were fixed with 10% neutral formalin buffer. After fixation, the samples were dehydrated and embedded in paraffin. The embedded samples were cut into 5-μm slices and stained with hematoxylin and eosin (H&E). Lesions in lung were observed by optical microscopy. Lung injury were determined through the severity of pneumonia in a blinded fashion [21].

After rehydrated through a graded series of alcohol, the slices were incubated with rabbit antibodies against HMGB-1 (1:200 diluted) and TLR4 (1:250 diluted) at 4°C overnight. The sections were then incubated with special HRP-conjugated goat anti-rabbit IgG antibody at 37°C for 30 minutes. Slides were stained with chromogenic substrate solution diaminobezidin (DAB) and counterstained with hematoxylin. The expression of HMGB-1 and TLR4 were visualized under a microscope [23].

Determination of lung virus titer

The frozen lung tissues were thawed and homogenized in PBS at a concentration of 100 mg tissue/1 mL PBS. The supernatant was split into small parts and stored at -80°C for subsequent use.

MDCK cells were plated at 2×10^6 cells in 96 cell plate till the cells grown to 90% confluent, cells were then infected with serial dilutions of supernatant from lung homogenate and incubated for 2 h at 37°C with 5% CO_2. The supernatant was removed and the wells were washed with PBS and incubated with 200 μL DMEM at 37°C, 5% CO_2 for 3 days. The cell activity was assessed by MTT assays. The lung virus titer was expressed by the inhibition rate of virus replication [24].

Anti-oxidant capacity in supernatant of lung homogenate

The anti-oxidation of INAE was tested through methods of ferric ion reducing antioxidant power (FRAP) kit. Levels of MPO and MDA, oxidant stress products in lung homogenate of IAV infected mice were evaluated by ELISA kits according to the manufacturer's instructions.

Assessment of cytokines in supernatant of lung homogenate

Levels of IFN-α, IFN-β, IFN-γ, MCP-1, RANTES, IP-10, TNF-α, IL-6, and IL-10 in the supernatant of lung homogenates were determined with ELISA kits according to the manufacturer's instructions.

Statistical analysis

All parameters were recorded for individuals within all groups and statistical computations were performed with GraphPad prism 6 (GraphPad software Inc., San Diego, CA, USA). Data comparison were carried out with one-way ANOVA and expressed as mean ± S.D. (Standard deviation). Post hoc comparisons were performed using Fishers's PLSD if any significant changes were found. The *P* values less than 0.05 were considered as statistically significant.

Results

Anti-influenza effect of INAE in vitro

The result showed that INAE had no toxicity on MDCK cells up to concentration of 1000 μg/mL (data not shown). As shown in Fig. 1A, INAE (100, 200, 400 μg/mL) was administrated 2 h before virus infection, virus replication was significantly inhibited. No obvious inhibition was observed on the cells treated with virus mix-incubated INAE simultaneously or with INAE 2 h after virus infection.

INAE inhibited NO production of macrophage *in vitro*

LPS stimulation increased NO production in peritoneal macrophages. As shown in Fig.1B, INAE remarkable suppressed the elevated NO production ($P < 0.05$).

inAE improved lifespan and survival rate of IAV infected mice

The experimental mice infected with IAV were observed for 14 days. The mice showed clinical signs of piloerection, ruffled fur, lack of food consumption, and body weight loss after virus inoculation. INAE significantly expanded lifespan of IAV infected mice (Fig.2A). Model group mice had a notable low survival time (8.30 ± 0.67 days) compared with INAE groups mice (ranged from 9.80 ± 2.12 days to 10.80 ± 2.66 days).

There was no death in the normal group during 14-day's observation. Model group mice were found dead since the 7^{th} day after infection and 100% of the model mice died within 9 days (Fig.2B). The survival rate of model group was 0% from the 9^{th} day. Mice treated with INAE (40, 80 and 160 mg/kg) were protected from lethality. When compared with model group, the survival rate of mice significantly raised in INAE 40 and 80 mg/kg groups during days 8 ~ 9 ($P < 0.05$), and in INAE 160 mg/kg group during days 8 ~ 12 ($P < 0.05$). The survival rate of INSE (40, 80 and 160 mg/kg) on 14^{th} day were 10%, 10%, and 20%.

Animal body temperature was also reported during the study. More interesting, body temperature of mice in model was lower than normal group, while INAE treatment groups exhibited higher temperature than model group (Fig.2C).

INAE alleviated acute lung injury in IAV infected mice

Pathologic findings indicated that normal group mice had lungs in terms of nature size, color, and texture with clear and intact round alveolar cells (Fig.3A). In the contrary, large areas of alveolar cells and bronchioles were damaged and most alveolar walls were destroyed in model group. Amounts of inflammatory cells infiltration was observed in injured alveolus and pneumocytes drop off from bronchiole. As shown in Fig.3A, histological damages in lung of mice were obviously alleviated in INAE treated groups. Inflammatory cell infiltration was significantly decreased compared with model group.

Body weight loss and lung index increase were also used to evaluate lung damage caused by influenza virus in mice. Remarkable increase was observed in lung index of model group (10.78 ± 0.93 mg/g).

Comparatively, treatment with INAE (Fig.3B) significant decreased the lung index (80 mg/kg, 9.25 ± 1.39 mg/g; 160 mg/kg, 8.34 ± 0.72 mg/g).

As shown in Fig.3C, IAV infected mice began to lose body weight since the 2nd day after infection. Compared to model group, the body weight of the mice treated with INAE and ribavirin were significantly higher on the 3rd day and the 4th day ($P < 0.05$).

Meanwhile, weights of liver, thymus and spleen in infected mice were significantly decreased compared with normal group. Comparatively, INAE administration (40, 80 and 160 mg/kg) significant increased weights and organ index of liver, and 160 mg/kg of INAE significantly increased both weight, organ indexes of spleen and thymus (Fig.4).

INAE inhibited virus titer in lung of IAV infected mice

Acute lung injury referred to virus replication and virus titer were determined by TCID50. As shown in Fig.3D, lung virus titer of mice which were treated with INAE (40 mg/kg, 3.78 ± 0.15; 80 mg/kg, 3.50 ± 0.20; 160 mg/kg, 2.87 ± 0.12) and ribavirin (2.36 ± 0.14) were clearly lower than that of model group (4.78 ± 0.16) on the 4th day after IAV infection ($P < 0.05$). The result suggested that the decrease of virus titer was accordance with the protective effect of INAE on lung injury.

INAE suppressed the expression of HMGB-1 and TLR4 in lung of IAV infected mice

As shown in Fig.5, mice in normal group basically expressed HMGB1 in nuclei of lung tissue. Compared with normal group, the expression of HMGB1 in model group increased and a large amount of HMGB1 was found out of nuclei and cells. INAE and ribavirin reduced the over expression and the release of HMGB1. Mice in normal group expressed a small quantity TLR4, while the expression increased in model group. The INAE and ribavirin treatment reduced TLR4 expression in renal tissue.

Anti-oxidant effect of INAE

As shown in Fig.6, the levels of MPO and MDA in lung were significantly increased in model group compared with normal group ($P < 0.05$). In comparison with model group, INAE administration markedly reduced MPO and MDA ($P < 0.05$). MPO, and MDA level were decreased in INAE treated mice compared with model group, which demonstrated the increased anti-oxidant capacity after INAE treatment.

INAE regulated cytokines expression in lung of IAV infected mice

As shown in Fig.7, the levels of IFN-α, IFN-β in lung were significantly increased in model group compared with normal group ($P < 0.05$). In comparison with model group, INAE administration markedly reduced IFN-α and IFN-β production ($P < 0.05$). The levels of IFN-γ was significantly decreased in model group compared and INAE administration markedly increased IFN-γ production ($P < 0.05$). Moreover, in comparison with normal group, model group exhibited significant increase in the levels of MCP-1, RANTES, IL-6 and TNF-α. After administration of INAE and ribavirin, the levels of proinflammatory

cytokines (MCP-1, RANTES, IL-6 and TNF-α) were remarkable decreased compared with model group ($P < 0.05$).

IP-10 is a chemokine mainly produced by mononuclear macrophages and T lymphocytes which highly increased in virus infected tissues. Our experiment showed that the level of IP-10 significantly increased in model group when compared with normal group ($P < 0.05$). Administration of INAE remarkably decreased IP-10 production in IAV infected mice ($P < 0.05$). IL-10 is an important anti-inflammatory factor that can ameliorate immunopathology by limiting innate and adaptive responses involved in tissue damage. The level of IL-10 was significantly decreased in lung of model mice when compared with mice in normal group. The administration of INAE significantly increase IL-10 production in lungs of IAV infected mice ($P < 0.05$).

Discussion

Traditional Chinese medicine, the precious treasure of China which stem from antique Chinese culture 2000 years ago, are used to treat diseases in China and southeast Asia [13]. Many traditional Chinese herbs, for instance, *Radix isatidis* (Banlangen), *Houttuynia cordata* (Yuxingcao), *Radix Scutellariae* (Huangqin)*,Folium isatidis* (Daqingye) were proved to exhibit anti-virus effect during pandemics of SARS in 2003 [25-27]. During the treatment period of COVID-19, TCM scheme was included in the guideline on diagnosis and treatment of COVID-19, and TCM fully participate in the whole rescue process [14]. Decoction is the main form of traditional Chinese medicine [28]. Yin-Ku Lin *et al. found that* the abstracts of Indigo naturalis in oil reduced the Nail Psoriasis Severity Index in patient, and the abstracts of Indigo naturalis in dimethyl sulfoxide inhibited suppressed the increase of protein carbonyl groups in human keratinocytes [29, 30]. However, as the main therapeutic dosage form of traditional Chinese medicine, rare research regarding the decoction of indigo naturalis has been seen on the acute lung injury induced by influenza A virus. In our study, INAE as the aqueous extract of indigo naturalis referred to clinical use of traditional Chinese medicine.

After herbal extract preparation, the constituents of INAE was analyzed using an UPLC-ESI-LTQ-MS system. In the experiment, more plentiful chromatographic peaks were detected in positive mode than in negative mode, and positive mode was chosen to characterize the chemical constituents of INAE. According to the retention times and m/z values of the molecular ions, 16 chemicals, including 9 alkaloids, 3 nucleosides, 2 amino acids, 1 terpene and 1 organic acid, were identified through the comparison with the standard compounds and the database of known chemicals (data showed in supplementary material Fig.S1 and Tab S1). Among these chemicals, alkaloids were the main small molecule in indigo naturalis [31, 32]. Alkaloids has been proven to exhibit antiviral efficacy and inhibit LPS induced inflammation [33, 34].

INAE were inoculated 2 h before, at the same time, or 2 h after IAV infection with MDCK cells to test the ani-virus efficacy in three different phases. *In vitro* results shown that INAE markedly inhibited virus

adhesion to cells when administrated before virus infection. INAE suppressed the elevated NO production from LPS-stimulated peritoneal macrophages.

The model of acute lung injury induced by IAV is usually used for research of anti-influenza agents. Once mice were infected with IAV, amounts of influenza virus infecting pneumocytes results in cells necrosis and apoptosis in lung tissues and causes acute lung injury [35, 36]. Disorder of balance between inflammation and anti-inflammation led to death of mice for the reason of continuous injury of lung and other organs [37, 38]. In our study, severe injury of vital organs, including weight decrease and organ indexes of liver, spleen and thymus were observed in IAV-infected mice on day 4. Administration of INAE alleviated injury of the vital organs, especially decreased lung weight and lung index, increased liver weight and liver index. Spleen and thymus injury were also released in high group of INAE treatment. Like influenza virus infection, liver demonstrated diffuse mononuclear and hepatic necrosis, and splenic tissue were shown to be atrophic in the current outbreak of COVID-19 infected patient [9, 39]. Most of the recommended prescriptions consists traditional Chinese medicines, which have the efficacy of heat-clearing and detoxicating. Indigo naturalis also has the similar feature, which provide a possibility that INAE might make contribution to attenuate vital organs injury in COVID-19 and more researches are needed for further discovery.

In our study, treatment with INAE significantly expanded the lifespan and increased the survival rate of IAV infected mice. Oral administration of INAE significant alleviated lung injury with reduced lung index and virus titer, as well as decreased inflammatory cells infiltration. Our study results that can alleviate acute lung injury is accordance with clinic treatment.

During the process of virus infection, amounts of HMGB-1 were released into the infected tissues due to tissue injury [40]. HMGB-1 was implicated in host tissue destruction and persistent pathological changes in IAV-infected hosts [41]. HMGB-1 is a crucial mediator in the pathogenesis of several viral infections, it can be released passively from necrotic cells and/or actively secreted by macrophages or monocytes into the extracellular milieu [42]. As a ligand of TLR4, HMGB-1 can activate alveolar macrophages to produce proinflammatory cytokines and induce ALI [43, 44]. TLR4, one of the important inflammatory signal receptors of the pathogen recognition receptors family (PRR), plays a critical role in the activation of innate and adaptive immune system as influenza virus and COVID-19 invasion [45]. TLR4 is also an important transmembrane protein for the development of cytokines production [46]. There is growing evidence that TLR4 signal inhibition alleviated lung injury in IVA infected mice [47, 48]. Our experiment demonstrated that INAE obviously inhibited over expression of HMGB-1 and TLR4 that might benefit the alleviation of lung injury in IAV infected mice.

Some cases showed neutrophil infiltration was related to cytokine storm [39]. FRAP is a global indicator of antioxidant capacity [49]. Myeloperoxidase (MPO) is an enzyme mainly found in azurophilic granules of neutrophils, which serves as a good marker of inflammation, tissue injury and neutrophil infiltration [50, 51]. Oxidative damage may represent crucial pathogenic factor in acute lung injury due to the increased production of reactive oxygen and nitrogen species [52]. MDA is the main products of lipid

peroxidation and mediate inflammation [53]. Treatment with INAE increased FRAP, and decreased MPO, MDA in lung of IAV infected mice, which demonstrated that INAE obviously increased total anti-oxidant capacity and suppressed oxidant stress.

Excessive production of proinflammatory factors plays a critical role in the pathogenesis of influenza virus infection. Lung damage and clinic symptoms associated with aberrant and uncontrolled cytokine production could ultimately lead to death [54, 55]. IL-6 and TNF-α were the early immune cytokines contribute to the proinflammatory production [56, 57]. MCP-1 and RANTES are the main chemokines during early infection stage of influenza [38, 58, 59]. IL-10 was a critical protective modulator which attenuated the activation of lymphocytes and inflammatory cascades during virus infection [60]. IP-10 belonged to the chemokine CXC subfamily and acted as a chemo attractor for T cells and NK cells [61, 62]. Importantly, a research demonstrated that induction of IP-10 in lung attracted pulmonary neutrophils, and led to lung inflammation during influenza infection [63]. Increasing IP-10 induction was consistently found in the serum of H5N1-infected patients and animal models including mice, ferrets and macaques [64]. The present study demonstrated that treatment with INAE remarkable modulated levels of antivirus factors (IFN-α, IFN-β and IFN-γ), decreased levels of chemokines MCP-1, RANTES and IP-10, and reduced the production of proinflammatory factors IL-6 and TNF-α. Meanwhile, INAE significantly increased the production of anti-inflammatory factor (IL-10).

Conclusion

In summary, our investigation described the beneficial effect of indigo naturalis against ALI in IAV infected mice, and the underlying mechanism might be closely associated with its inhibition of virus replication, anti-inflammatory and anti-oxidant effect (Fig. 8). As acute lung injury, dysfunction of other vital organs such as liver, spleen and thymus were occurred and propagated in both influenza virus and SARS-CoV-2, our study suggested Indigo naturalis could be a promising agent and warrant further evaluation for the treatment of influenza A virus induced acute lung injury and SARS-CoV-2 induced COVID-19.

Abbreviations

INAE: Aqueous extract of indigo naturalis; ALI: Acute lung injury; IAV: Influenza A virus; HMGB-1: High mobility group box-1 protein; TLR4: Toll-like receptor 4; LD_{50}: 50% of lethal dose; MDCK: Madin-Darby canine kidney; DMEM: Dulbecco's modified Eagle's medium; MTT: 3-(4,5-dimethyl-2-thiazolyl)-2,5-diphenyl-2-H-tetrazolium bromide; OD: Optical density; CMC-Na: Carboxymethyl cellulose sodium; DAB: Diaminobezidin; FRAP: Ferric ion reducing antioxidant power; IFN-α: Interferon α; IFN-β: Interferon β; IFN-γ: Interferon γ; MCP-1: Monocyte chemoattractant protein-1; RANTES: Regulated upon activation normal T cell expressed and secreted factor; IP-10: Interferon induced protein-10; TNF-α: Tumor necrosis factor-α; IL-6: Interleukin-6; IL-10: Interleukin-10; MPO: Myeloperoxidase; MDA: Malonaldehyde; NO: Nitrogen oxide; lipopolysaccharide (LPS); H&E: Hematoxylin and eosin; ANOVA: One-way analysis of variance.

Declarations

Acknowledgements

Not applicable.

Authors’ contribution

Daofeng Chen conceived and design the work. Hong Li, Yunyi Zhang, Yan Lu and Haiyan Zhu contributed to study design of immunology, antivirus and chemistry, and development of the study protocol. Rong Tian contributed to the chemistry analysis. Lijun Ling contributed to in vivo experiment. Peng Tu takes responsibility for the integrity of the work as a whole, from inception to publication. All authors had read and approved the submitted version of the manuscript.

Funding

This work was supported by the National Key R&D Program of China (grant No. 2019YFC 1711000) and the National Natural Science Foundation of China (grant No.81330089).

Availability of data and materials

The datasets used and/or analyzed during the current study are available from the corresponding author on reasonable request.

Ethics approval and consent to participate

The study on animal was approved by the animal ethical committee of school of pharmacy, Fudan University (approval No. 2015-10-SY-CDF-01).

Consent for publication

Not applicable.

Competing interests

The authors declare that there are no conflicts of interest regarding the publication of this article.

Author details

1. *Department of Natural Medicine, School of Pharmacy, Fudan University, Shanghai, 201203, P. R. China*
2. *Department of Pharmacology, School of Pharmacy, Fudan University, Shanghai, 201203, P. R. China*
3. *Department of Microbiological and Biochemical Pharmacy, School of Pharmacy, Fudan University, Shanghai, 201203, P. R. China*

References

1. Li K, Hao Z, Zhao X*, et al.* SARS-CoV-2 infection-induced immune responses: Friends or foes? [J]. *Scand J Immunol*, 2020: e12895.
2. Martini M, Gazzaniga V, Bragazzi NL*, et al.* The Spanish Influenza Pandemic: a lesson from history 100 years after 1918 [J]. *J Prev Med Hyg*, 2019, **60**(1): E64-e67.
3. Zhang G-b, Tian L-q, Li Y-m*, et al.* Protective effect of homonojirimycin from Commelina communis (dayflower) on influenza virus infection in mice [J]. *Phytomedicine*, 2013, **20**(11): 964-968.
4. Webster RG, Bean WJ, Gorman OT*, et al.* Evolution and ecology of influenza A viruses [J]. *Microbiological reviews*, 1992, **56**(1): 152-179.
5. Lamb RA and Choppin PW. The gene structure and replication of influenza virus [J]. *Annual review of biochemistry*, 1983, **52**(1): 467-506.
6. Yewdell J and García-Sastre A. Influenza virus still surprises [J]. *Current opinion in microbiology*, 2002, **5**(4): 414-418.
7. Boltz DA, Aldridge JR, Webster RG*, et al.* Drugs in development for influenza [J]. *Drugs*, 2010, **70**(11): 1349-1362.
8. Yu C, Yan Y, Wu X*, et al.* Anti-influenza virus effects of the aqueous extract from Mosla scabra [J]. *Journal of ethnopharmacology*, 2010, **127**(2): 280-285.
9. McMullen SM, Meade M, Rose L*, et al.* Partial ventilatory support modalities in acute lung injury and acute respiratory distress syndrome-a systematic review [J]. *PLoS One*, 2012, **7**(8): e40190.
10. Damgaard C, Reinholdt J, Palarasah Y*, et al.* In vitro complement activation, adherence to red blood cells and induction of mononuclear cell cytokine production by four strains of Aggregatibacter actinomycetemcomitans with different fimbriation and expression of leukotoxin [J]. *J Periodontal Res*, 2017, **52**(3): 485-496.
11. Rattan A, Pawar SD, Nawadkar R*, et al.* Synergy between the classical and alternative pathways of complement is essential for conferring effective protection against the pandemic influenza A(H1N1) 2009 virus infection [J]. *PLoS Pathog*, 2017, **13**(3): e1006248.
12. Garg S, Garg M, Prabhakar N*, et al.* Unraveling the mystery of Covid-19 cytokine storm: From skin to organ systems [J]. *Dermatol Ther*, 2020: e13859.
13. Xie Q-F, Xie J-H, Dong TTX*, et al.* Effect of a derived herbal recipe from an ancient Chinese formula, Danggui Buxue Tang, on ovariectomized rats [J]. *Journal of ethnopharmacology*, 2012, **144**(3): 567-575.

14. Ren JL, Zhang AH and Wang XJ. Traditional Chinese medicine for COVID-19 treatment [J]. *Pharmacol Res*, 2020, **155**: 104743.
15. Commission CP. Chinese pharmacopoeia [J]. *China Medical Science Press, Beijing*, 2010, **228**.
16. Hsieh W-L, Lin Y-K, Tsai C-N*, et al.* Indirubin, an acting component of indigo naturalis, inhibits EGFR activation and EGF-induced CDC25B gene expression in epidermal keratinocytes [J]. *Journal of dermatological science*, 2012, **67**(2): 140-146.
17. Lin Y-K, Leu Y-L, Yang S-H*, et al.* Anti-psoriatic effects of indigo naturalis on the proliferation and differentiation of keratinocytes with indirubin as the active component [J]. *Journal of dermatological science*, 2009, **54**(3): 168-174.
18. Lin SC, Kappes MA, Chen MC*, et al.* Distinct susceptibility and applicability of MDCK derivatives for influenza virus research [J]. *PLoS One*, 2017, **12**(2): e0172299.
19. Huang D, Peng WJ, Ye Q*, et al.* Serum-Free Suspension Culture of MDCK Cells for Production of Influenza H1N1 Vaccines [J]. *PLoS One*, 2015, **10**(11): e0141686.
20. Larson KC, Lipko M, Dabrowski M*, et al.* Gng12 is a novel negative regulator of LPS-induced inflammation in the microglial cell line BV-2 [J]. *Inflamm Res*, 2010, **59**(1): 15-22.
21. Zhu H, Lu X, Ling L*, et al.* Houttuynia cordata polysaccharides ameliorate pneumonia severity and intestinal injury in mice with influenza virus infection [J]. *J Ethnopharmacol*, 2018, **218**: 90-99.
22. Zhi HJ, Zhu HY, Zhang YY*, et al.* In vivo effect of quantified flavonoids-enriched extract of Scutellaria baicalensis root on acute lung injury induced by influenza A virus [J]. *Phytomedicine*, 2019, **57**: 105-116.
23. Xu YY, Zhang YY, Ou YY*, et al.* Houttuyniacordata Thunb. polysaccharides ameliorates lipopolysaccharide-induced acute lung injury in mice [J]. *J Ethnopharmacol*, 2015, **173**: 81-90.
24. Chen Z, Santos C, Aspelund A*, et al.* Evaluation of live attenuated influenza a virus h6 vaccines in mice and ferrets [J]. *J Virol*, 2009, **83**(1): 65-72.
25. Lau K-M, Lee K-M, Koon C-M*, et al.* Immunomodulatory and anti-SARS activities of Houttuynia cordata [J]. *Journal of ethnopharmacology*, 2008, **118**(1): 79-85.
26. Lau T, Leung P, Wong E*, et al.* Using herbal medicine as a means of prevention experience during the SARS crisis [J]. *The American journal of Chinese medicine*, 2005, **33**(03): 345-356.
27. Peng J, Fan G and Wu Y. Isolation and purification of clemastanin B and indigoticoside A from Radix Isatidis by high-speed counter-current chromatography [J]. *Journal of Chromatography A*, 2005, **1091**(1): 89-93.
28. Naganuma M, Sugimoto S, Mitsuyama K*, et al.* Efficacy of indigo naturalis in a multicenter randomized controlled trial of patients with ulcerative colitis [J], 2018, **154**(4): 935-947.
29. Lin YK, See LC, Huang YH*, et al.* Efficacy and safety of Indigo naturalis extract in oil (Lindioil) in treating nail psoriasis: a randomized, observer-blind, vehicle-controlled trial [J]. *Phytomedicine*, 2014, **21**(7): 1015-1020.

30. Lin YK, Chen HW, Yang SH*, et al.* Protective effect of indigo naturalis extract against oxidative stress in cultured human keratinocytes [J]. *J Ethnopharmacol*, 2012, **139**(3): 893-896.
31. Liu Z, Yang ZQ and Xiao H. Antiviral activity of the effective monomers from Folium Isatidis against influenza virus in vivo [J]. *Virol Sin*, 2010, **25**(6): 445-451.
32. Jiang L, Lu Y, Jin J*, et al.* n-Butanol extract from Folium isatidis inhibits lipopolysaccharide-induced inflammatory cytokine production in macrophages and protects mice against lipopolysaccharide-induced endotoxic shock [J]. *Drug Des Devel Ther*, 2015, **9**: 5601-5609.
33. Cecil CE, Davis JM, Cech NB*, et al.* Inhibition of H1N1 influenza A virus growth and induction of inflammatory mediators by the isoquinoline alkaloid berberine and extracts of goldenseal (Hydrastis canadensis) [J]. *Int Immunopharmacol*, 2011, **11**(11): 1706-1714.
34. Zhao L, Wang L, Di SN*, et al.* Steroidal alkaloid solanine A from Solanum nigrum Linn. exhibits anti-inflammatory activity in lipopolysaccharide/interferon gamma-activated murine macrophages and animal models of inflammation [J]. *Biomed Pharmacother*, 2018, **105**: 606-615.
35. Sumikoshi M, Hashimoto K, Kawasaki Y*, et al.* Human influenza virus infection and apoptosis induction in human vascular endothelial cells [J]. *Journal of medical virology*, 2008, **80**(6): 1072-1078.
36. Teijaro John R, Walsh Kevin B, Cahalan S*, et al.* Endothelial Cells Are Central Orchestrators of Cytokine Amplification during Influenza Virus Infection [J]. *Cell*, 2011, **146**(6): 980-991.
37. Ciaglia E, Malfitano AM, Laezza C*, et al.* Immuno-Modulatory and Anti-Inflammatory Effects of Dihydrogracilin A, a Terpene Derived from the Marine Sponge Dendrilla membranosa [J]. *Int J Mol Sci*, 2017, **18**(8).
38. Van Reeth K. Cytokines in the pathogenesis of influenza [J]. *Veterinary microbiology*, 2000, **74**(1): 109-116.
39. Barnes BJ, Adrover JM, Baxter-Stoltzfus A*, et al.* Targeting potential drivers of COVID-19: Neutrophil extracellular traps [J]. *J Exp Med*, 2020, **217**(6).
40. lǔ *Shijinmo variorum of clinic practices with double-herb prescriptions* [M]. People's Medical Publishing House, 2002.
41. Zheng J and Perlman S. Immune responses in influenza A virus and human coronavirus infections: an ongoing battle between the virus and host [J]. *Curr Opin Virol*, 2018, **28**: 43-52.
42. Moisy D, Avilov SV, Jacob Y*, et al.* HMGB1 protein binds to influenza virus nucleoprotein and promotes viral replication [J]. *J Virol*, 2012, **86**(17): 9122-9133.
43. Deng Y, Yang Z, Gao Y*, et al.* Toll-like receptor 4 mediates acute lung injury induced by high mobility group box-1 [J]. *PLoS One*, 2013, **8**(5): e64375.
44. Fagone P, Shedlock DJ, Bao H*, et al.* Molecular adjuvant HMGB1 enhances anti-influenza immunity during DNA vaccination [J]. *Gene Ther*, 2011, **18**(11): 1070-1077.
45. Tao X, Sun X, Yin L*, et al.* Dioscin ameliorates cerebral ischemia/reperfusion injury through the downregulation of TLR4 signaling via HMGB-1 inhibition [J]. *Free Radical Biology and Medicine*,

2015, **84**: 103-115.

46. Wang QW, Su Y, Sheng JT*, et al.* Anti-influenza A virus activity of rhein through regulating oxidative stress, TLR4, Akt, MAPK, and NF-kappaB signal pathways [J]. *PLoS One*, 2018, **13**(1): e0191793.
47. Dai JP, Wang QW, Su Y*, et al.* Emodin Inhibition of Influenza A Virus Replication and Influenza Viral Pneumonia via the Nrf2, TLR4, p38/JNK and NF-kappaB Pathways [J]. *Molecules*, 2017, **22**(10).
48. Ren Z, Li J, Song X*, et al.* The regulation of inflammation and oxidative status against lung injury of residue polysaccharides by Lentinula edodes [J]. *Int J Biol Macromol*, 2018, **106**: 185-192.
49. Koivisto AE, Olsen T, Paur I*, et al.* Effects of antioxidant-rich foods on altitude-induced oxidative stress and inflammation in elite endurance athletes: A randomized controlled trial [J]. *PLOS ONE*, 2019, **14**(6): e0217895.
50. Phung TT, Luong ST, Kawachi S*, et al.* Interleukin 12 and myeloperoxidase (MPO) in Vietnamese children with acute respiratory distress syndrome due to Avian influenza (H5N1) infection [J]. *J Infect*, 2011, **62**(1): 104-106.
51. Kato Y. Neutrophil myeloperoxidase and its substrates: formation of specific markers and reactive compounds during inflammation [J]. *J Clin Biochem Nutr*, 2016, **58**(2): 99-104.
52. Das S and Kanodia L. Effect of ethanolic extract of leaves of Moringa olifera lam. on acetic acid induced colitis in albino rats [J]. *Asian J Pharm Clin Res*, 2012, **5**(3): 110-114.
53. Shema-Didi L, Sela S, Ore L*, et al.* One year of pomegranate juice intake decreases oxidative stress, inflammation, and incidence of infections in hemodialysis patients: a randomized placebo-controlled trial [J]. *Free Radical Biology and Medicine*, 2012, **53**(2): 297-304.
54. Peiris J, Hui KP and Yen H-L. Host response to influenza virus: protection versus immunopathology [J]. *Current opinion in immunology*, 2010, **22**(4): 475-481.
55. Ivashkiv LB and Donlin LT. Regulation of type I interferon responses [J]. *Nature reviews Immunology*, 2014, **14**(1): 36-49.
56. Szretter KJ, Gangappa S, Lu X*, et al.* Role of Host Cytokine Responses in the Pathogenesis of Avian H5N1 Influenza Viruses in Mice [J]. *Journal of virology*, 2007, **81**(6): 2736-2744.
57. Julkunen I, Sareneva T, Pirhonen J*, et al.* Molecular pathogenesis of influenza A virus infection and virus-induced regulation of cytokine gene expression [J]. *Cytokine & growth factor reviews*, 2001, **12**(2): 171-180.
58. Guo X-zJ and Thomas PG. New fronts emerge in the influenza cytokine storm [J]. *Seminars in Immunopathology*, 2017, **39**(5): 541-550.
59. Tavares LP, Teixeira MM and Garcia CC. The inflammatory response triggered by Influenza virus: a two edged sword [J]. *Inflammation Research*, 2017, **66**(4): 283-302.
60. Julkunen I, Melén K, Nyqvist M*, et al.* Inflammatory responses in influenza A virus infection [J]. *Vaccine*, 2000, **19**: S32-S37.
61. Neville LF, Mathiak G and Bagasra O. The immunobiology of interferon-gamma inducible protein 10 kD (IP-10): a novel, pleiotropic member of the C-X-C chemokine superfamily [J]. *Cytokine Growth*

Factor Rev, 1997, **8**(3): 207-219.

62. Moser M, Knoth R, Bode C*, et al.* LE-PAS, a novel Arnt-dependent HLH-PAS protein, is expressed in limbic tissues and transactivates the CNS midline enhancer element [J]. *Brain Res Mol Brain Res*, 2004, **128**(2): 141-149.
63. Ichikawa A, Kuba K, Morita M*, et al.* CXCL10-CXCR3 enhances the development of neutrophil-mediated fulminant lung injury of viral and nonviral origin [J]. *Am J Respir Crit Care Med*, 2013, **187**(1): 65-77.
64. Mok CK, Kang SS, Chan RW*, et al.* Anti-inflammatory and antiviral effects of indirubin derivatives in influenza A (H5N1) virus infected primary human peripheral blood-derived macrophages and alveolar epithelial cells [J]. *Antiviral Res*, 2014, **106**: 95-104.

Figures

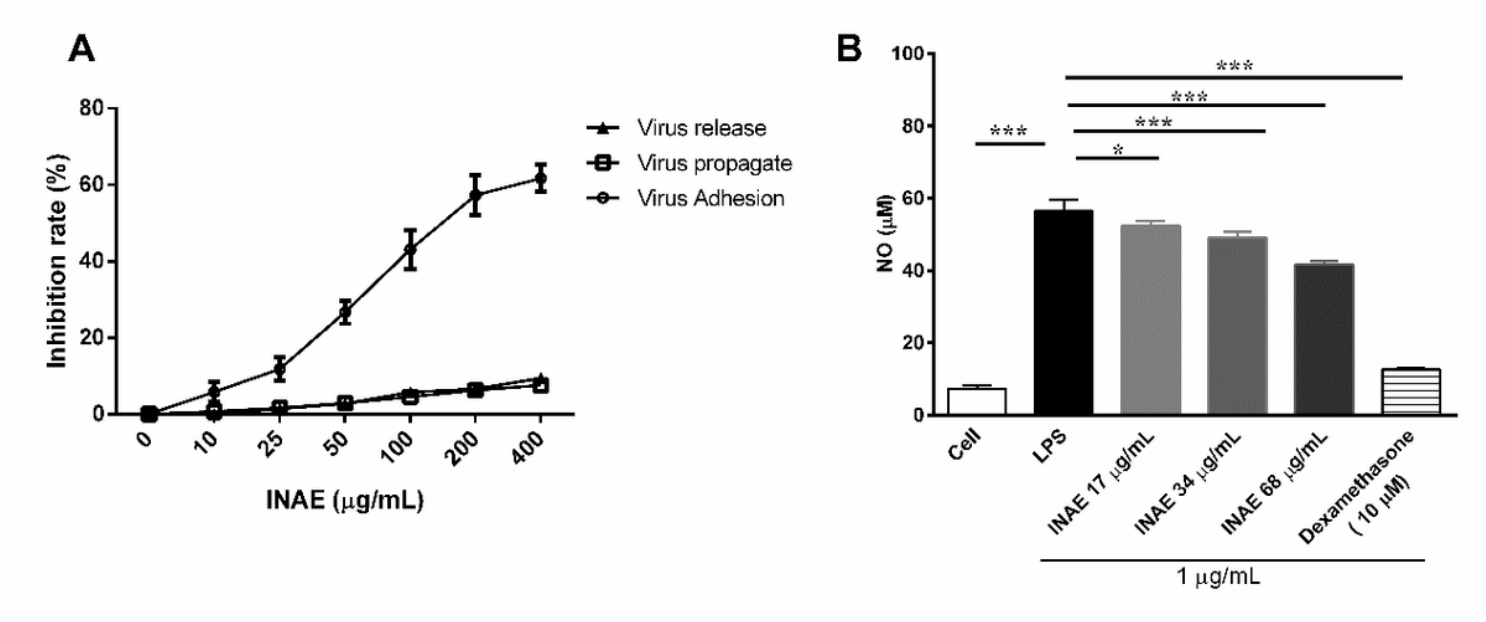

Figure 1

Anti-influenza virus and anti-inflammatory effect of INAE in vitro (A) Anti-influenza virus effect of INAE on MDCK cells. INAE was administrated 2 hours before, incubated with influenza virus at the same time, or 2 hours after influenza virus infection to evaluate the antivirus capacity in phases of virus adhesion, virus propagate or virus release. (B) Effect of INAE on LPS-induced nitric oxide (NO) production. LPS (1 μg/mL) was used as initiators in peritoneal macrophages and dexamethasone (10 μM) was used as positive control. Data were presented as mean ± S.D. (n = 4). * $P < 0.05$, *** $P < 0.001$ compared with LPS group, tested by ANOVA and Fisher's PLSD.

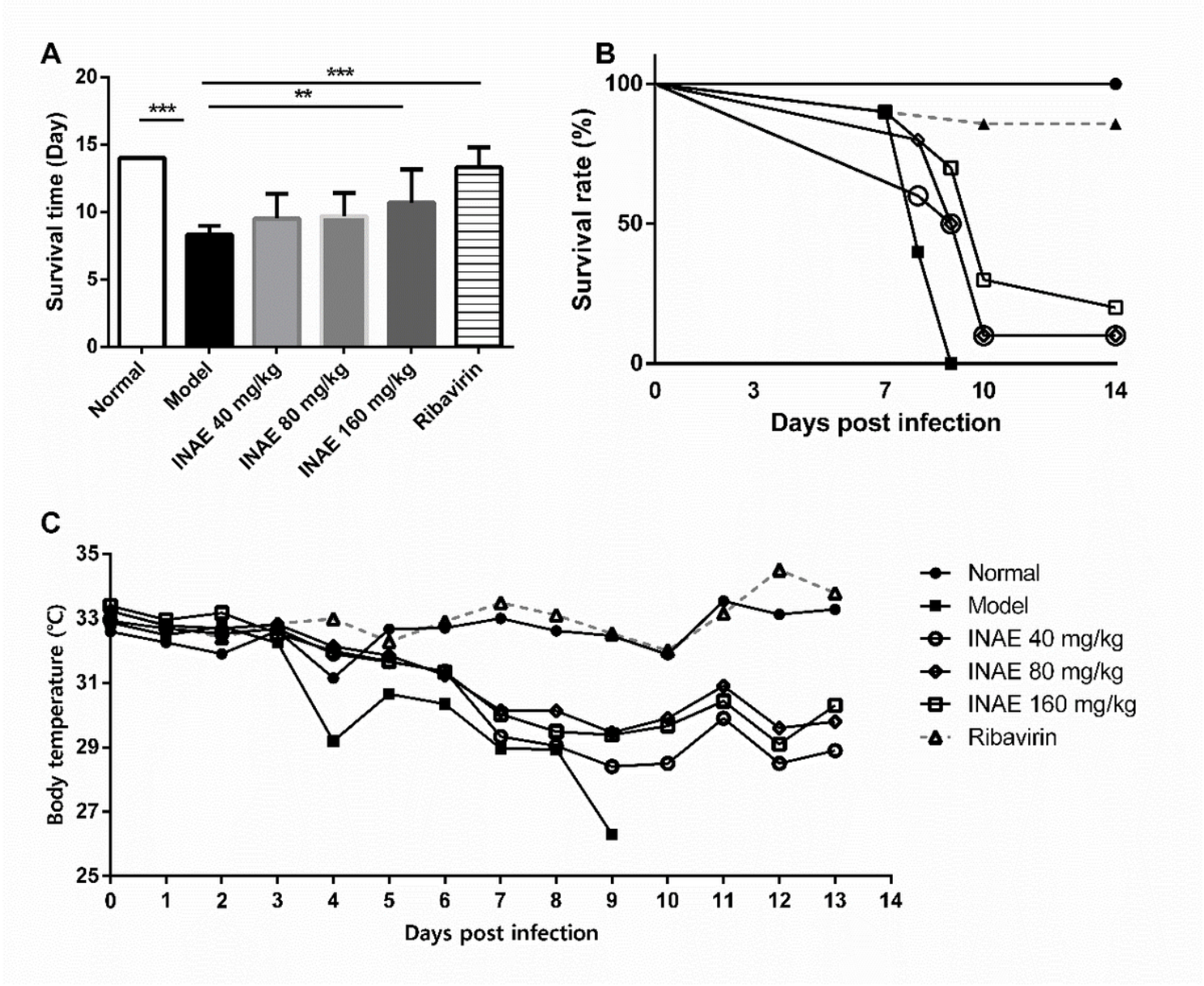

Figure 2

Effect of INAE on lifespan and survival rate of IAV infected mice Mice were intranasally infected with 6 × LD50 of IAV and orally administered with INAE, ribavirin or 0.5% CMC-Na at indicated doses once daily for 7 days. Mice lifespan (A), Survival rate (B), and Animal body mean temperature during the study (C) were recorded. Data represent were expressed as mean ± S.D. (n =7 ~ 10) ** P < 0.01, *** P < 0.001 compared with model group, tested by ANOVA and Fisher's PLSD.

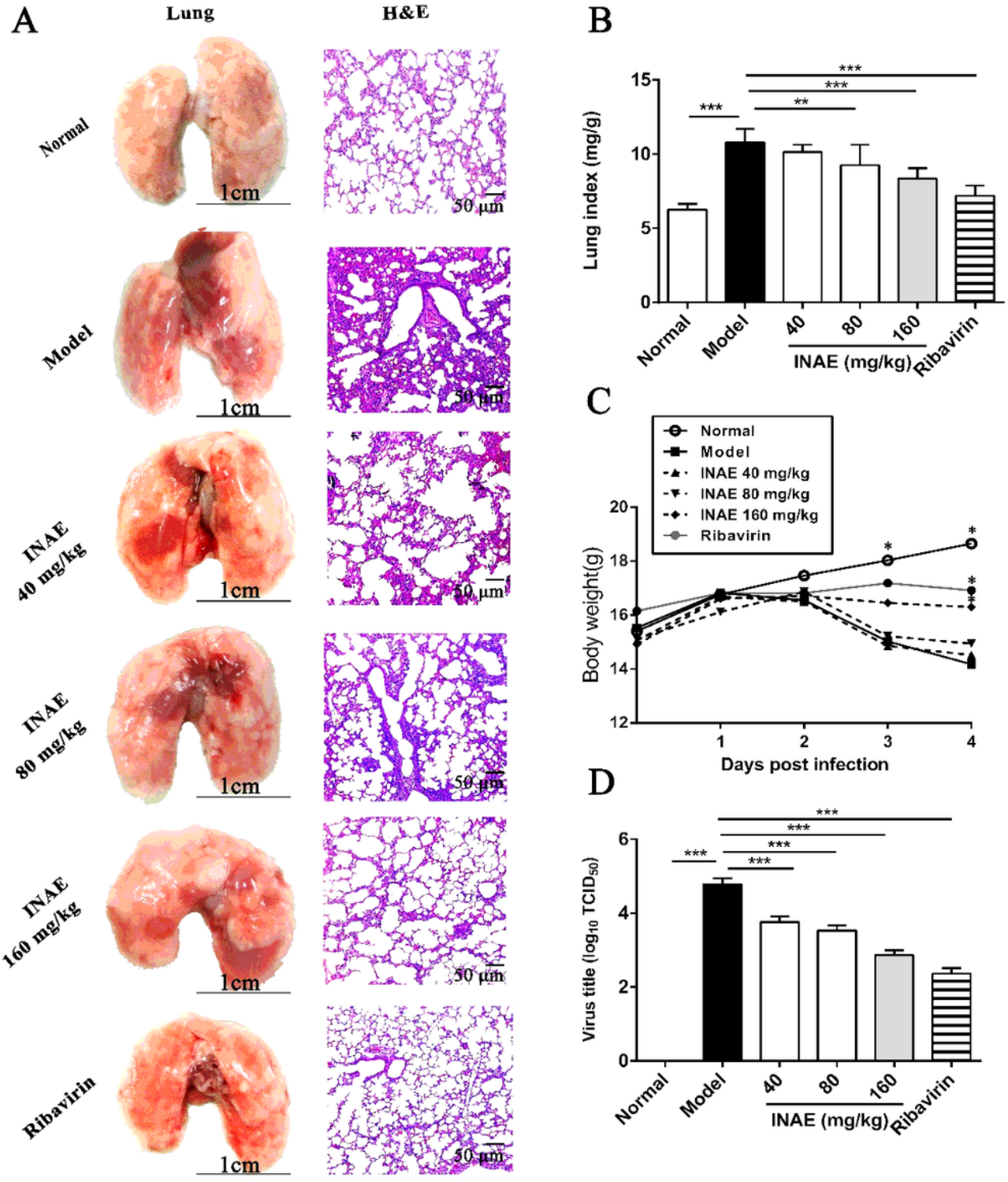

Figure 3

Effect of INAE on lung injury, lung index, body weight and virus titer of IAV infected mice Mice were infected with 3 × LD50 of IAV and orally administered INAE, ribavirin or 0.5% CMC-Na at indicated doses once daily for 4 days. Lung index, mice body weight, and virus titer were recorded. Lung photos and hematoxylin-eosin stain (H&E) with vision of 200 × (A). Lung index = Lung weight / body weight (B). Mice

body weight growth curve (C). Virus titer in lung of mice (D). Data were presented as mean ± S.D. (n =6). ** P < 0.01, *** P < 0.001 compared with model group, tested by ANOVA and Fisher's PLSD.

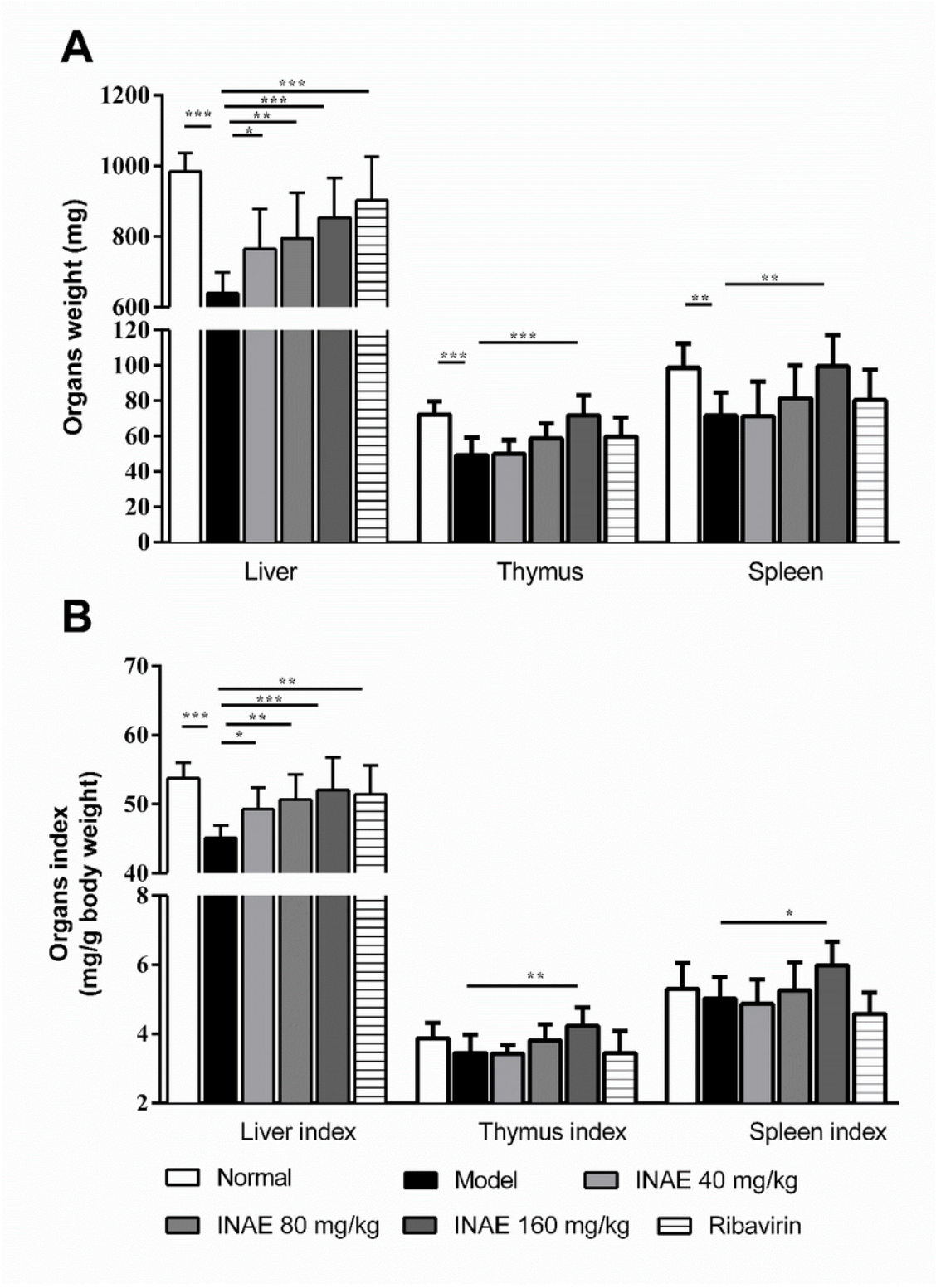

Figure 4

Effect of INAE on liver, thymus and spleen Mice were infected with 3 × LD50 of IAV and orally administered INAE, ribavirin or 0.5% CMC-Na at indicated doses once daily for 4 days. Weights of liver, thymus and spleen were measured and calculated (A ~ B). Organ index = Organ weight / body weight ×

100%. Data were presented as mean ± S.D. (n =6). * P < 0.05, ** P < 0.01, *** P < 0.001 compared with model group, tested by ANOVA and Fisher's PLSD.

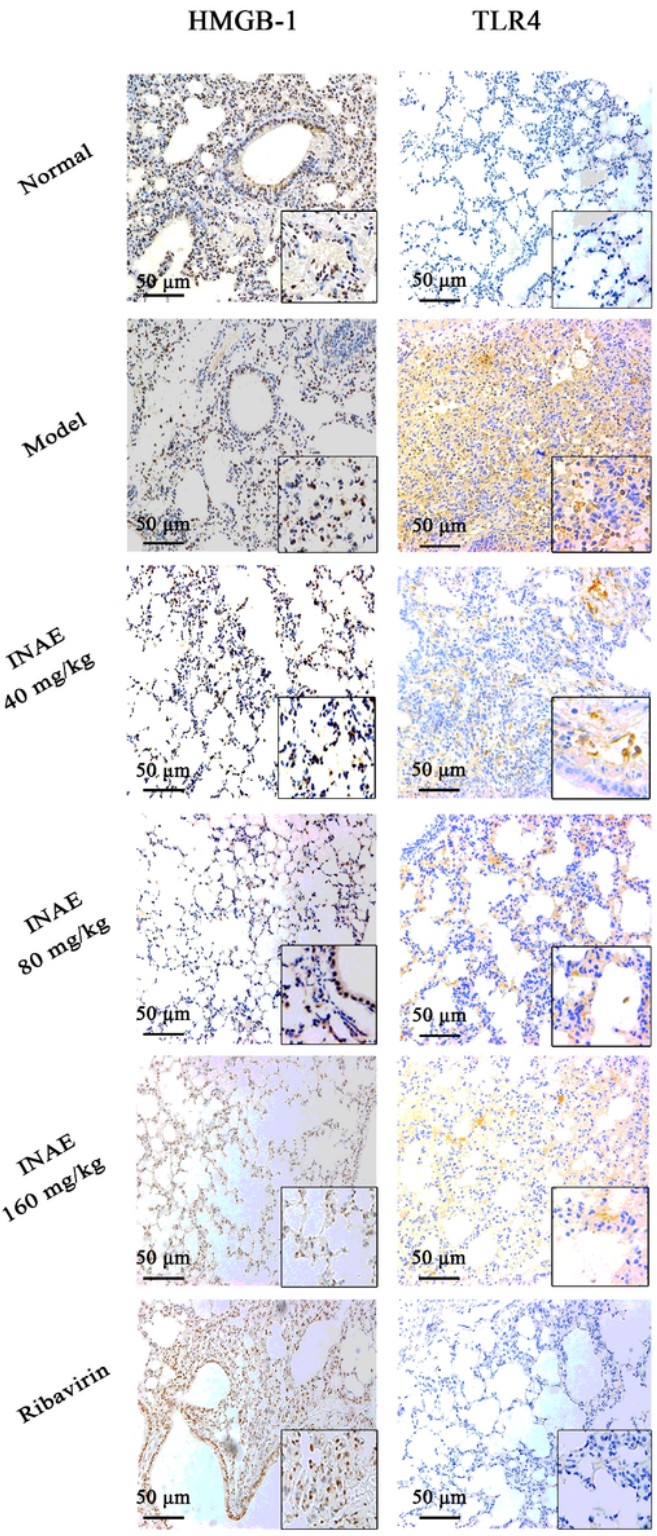

Figure 5

HMGB-1 and TLR4 expression in lung tissue of IAV infected mice The lung tissues of IAV infected mice were harvested, fixed in formalin, and embedded in paraffin for slices preparation. The slides were incubated with relative antibodies against HMGB-1 and TLR4, stained with chromogenic substrate

solution and counterstained with hematoxylin. The immuno-histochemical (200 ×) of expression of HMGB-1 and TLR4 in lung of IAV infected mice were visualized under a microscope.

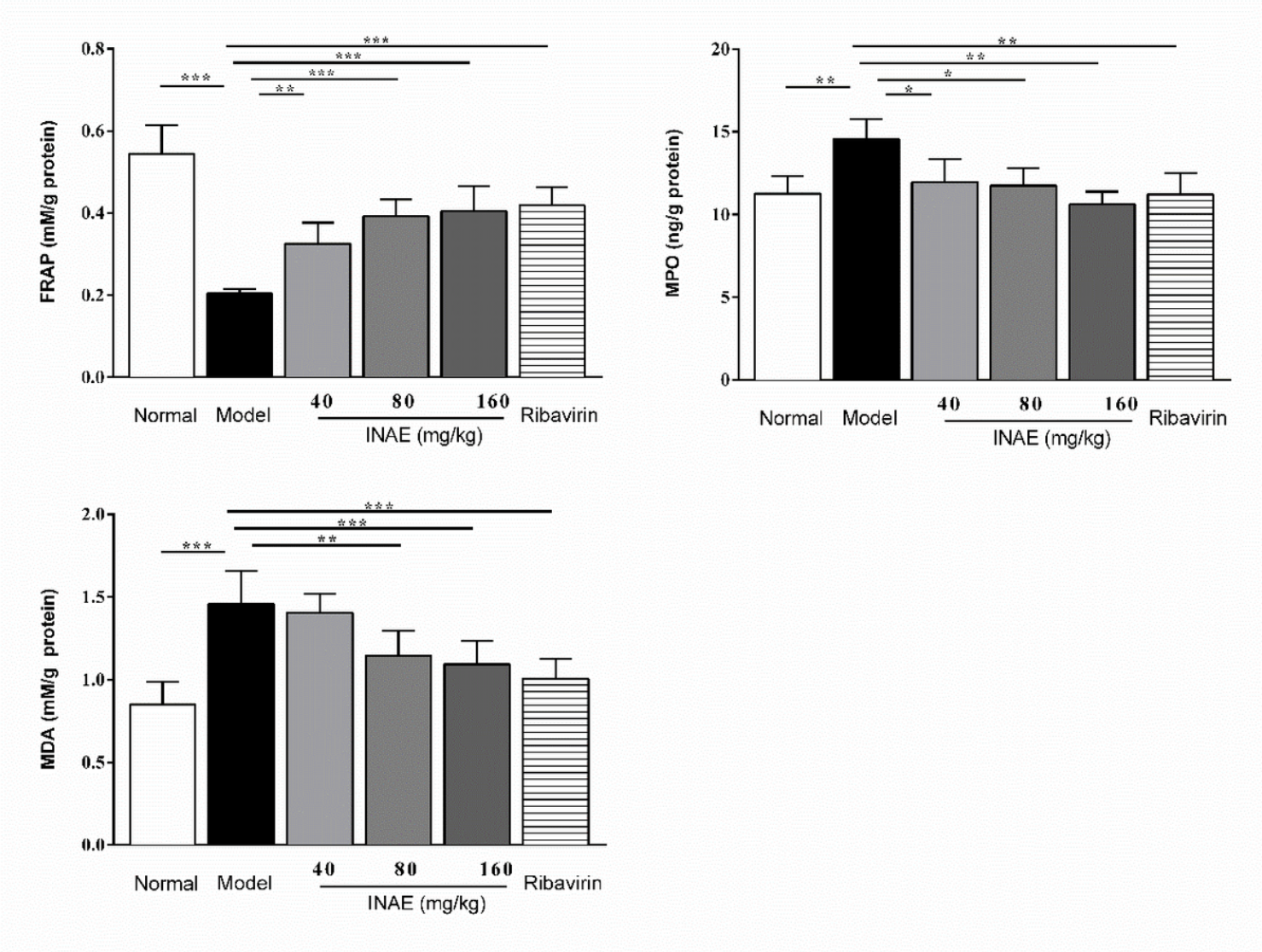

Figure 6

Anti-oxidant effect of INAE in lung of IAV-infected mice Effect of INAE on oxidant stress reaction in lung of IAV-infected mice at day 4 post infection. (A) Ferric ion reducing antioxidant power. (B) MPO. (C) MDA. Data were expressed as mean ± S.D. (n = 6). * $P < 0.05$, ** $P < 0.01$, *** $P < 0.001$ compared with model group, tested by ANOVA and Fisher's PLSD.

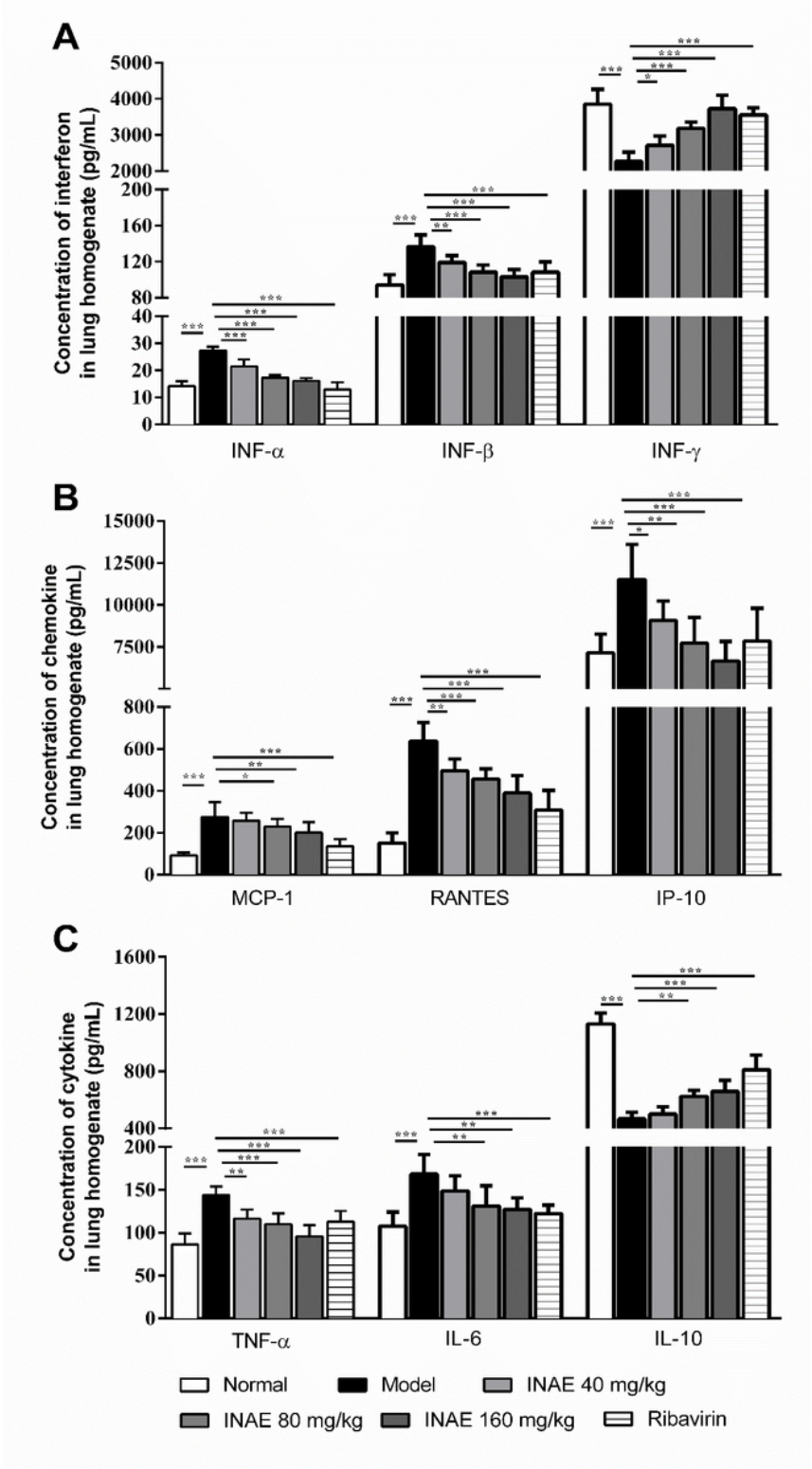

Figure 7

Interferon, chemokine and cytokine levels in lung of IAV infected mice Effect of INAE on cytokines production in lung of IAV-infected mice at day 4 post infection. Interferon IFN-α, IFN-β, and INF-γ (A), MCP-1, RANTES and IP-10 (B), and TNF-α, IL-6, and IL-10 (C) level were evaluated. Data were expressed as mean ± S.D. (n = 6). * $P < 0.05$, ** $P < 0.01$, *** $P < 0.001$ compared with model group, tested by ANOVA and Fisher's PLSD.

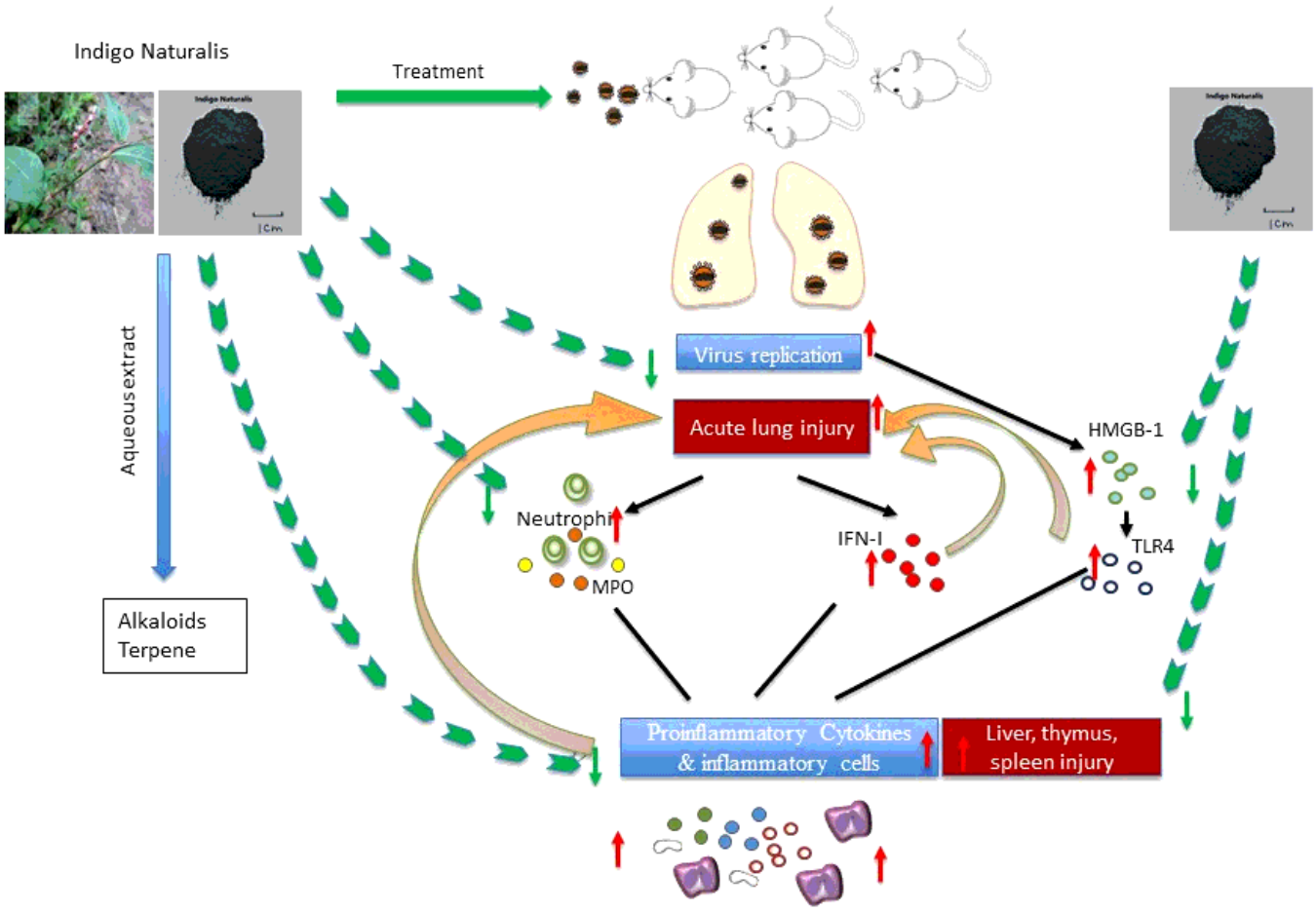

Figure 8

Graphic abstract of IAV induced acute lung injury. Influenza A virus infect host alveolar epithelial cells and cause necrosis and injury in lung. The innate immune response begins with the virus recognition of pathogen-associated molecular patterns through HMGB-1 and TLR4 pathway. Extensive cytokines and amounts of peroxide produced by neutrophils exacerbate the injury of lung, as well as the surrounding tissues and organs (red arrow). INAE treatment alleviated the acute lung injury (green arrow) through effects of anti-virus, anti-inflammatory and anti-oxidation.

Supplementary Files

This is a list of supplementary files associated with this preprint. Click to download.

- Supplymentmaterialforreview.doc